PCP
PLANT & CELL PHYSIOLOGY

Long-Distance Electrical and Calcium Signals Evoked by Hydrogen Peroxide in Physcomitrella

Mateusz Koselski[1,*], Sebastian N. W. Hoernstein[2], Piotr Wasko[1], Ralf Reski[2,3] and Kazimierz Trebacz[1]

[1]Department of Plant Physiology and Biophysics, Institute of Biological Sciences, Maria Curie-Skłodowska University, Akademicka 19, Lublin 20-033, Poland
[2]Plant Biotechnology, Faculty of Biology, University of Freiburg, Schaenzlestrasse 1, Freiburg 79104, Germany
[3]Signalling Research Centres BIOSS and CIBSS, Schaenzlestrasse 18, Freiburg 79104, Germany

*Corresponding author: E-mail, mateusz.koselski@poczta.umcs.lublin.pl

(Received 2 June 2022; Accepted 21 July 2023)

Regular Paper

Electrical and calcium signals in plants are some of the basic carriers of information that are transmitted over a long distance. Together with reactive oxygen species (ROS) waves, electrical and calcium signals can participate in cell-to-cell signaling, conveying information about different stimuli, e.g. abiotic stress, pathogen infection or mechanical injury. There is no information on the ability of ROS to evoke systemic electrical or calcium signals in the model moss Physcomitrella nor on the relationships between these responses. Here, we show that the external application of hydrogen peroxide (H_2O_2) evokes electrical signals in the form of long-distance changes in the membrane potential, which transmit through the plant instantly after stimulation. The responses were calcium-dependent since their generation was inhibited by lanthanum, a calcium channel inhibitor (2 mM), and EDTA, a calcium chelator (0.5 mM). The electrical signals were partially dependent on glutamate receptor (GLR) ion channels since knocking-out the *GLR* genes only slightly reduced the amplitude of the responses. The basal part of the gametophyte, which is rich in protonema cells, was the most sensitive to H_2O_2. The measurements carried out on the protonema expressing fluorescent calcium biosensor GCaMP3 proved that calcium signals propagated slowly (>5 μm/s) and showed a decrement. We also demonstrate upregulation of a stress-related gene that appears in a distant section of the moss 8 min after the H_2O_2 treatment. The results help understand the importance of both types of signals in the transmission of information about the appearance of ROS in the plant cell apoplast.

Keywords: Calcium imaging • Cell excitability • Cell-to-cell signaling • Glutamate receptor • Hydrogen peroxide • Stress-related genes

Introduction

As an early terrestrial plant, the moss Physcomitrella (new botanical name *Physcomitrium patens*) had to cope with exposure to UV radiation, ozone, wounding and many other abiotic and biotic stressors that enhance the synthesis of reactive oxygen species (ROS) (Tucker et al. 2005, Rensing et al. 2008, 2020). Physcomitrella is an emerging model plant with a fully sequenced genome (Rensing et al. 2008, Lang et al. 2018). It is widely used to study defense mechanisms against environmental stress factors (Frank et al. 2005, Saidi et al. 2009, Koselski et al. 2019, Hoernstein et al. 2023).

It was previously demonstrated in laboratory of Plant Physiology and Biophysics, Maria Curie-Sklodowska University, Lublin, Poland that Physcomitrella is capable of generating action potentials (APs) after illumination with light of sufficient (over-threshold) intensity, cooling, glutamate (Glu) treatment, etc. (Koselski et al. 2008, 2019, 2020). Electrophysiological experiments with the application of ion channel inhibitors and the manipulation of ion gradients across the plasma membrane indicated that Ca^{2+} fluxes from external and internal stores were involved in the generation of APs in Physcomitrella. They interacted with K^+ and, to a lesser extent, with Cl^- fluxes. Our recent study on GCaMP mutants allowing the monitoring of changes in the cytoplasmic Ca^{2+} concentration ($[Ca^{2+}]_{cyt}$) demonstrated that the local Glu application caused an increase in $[Ca^{2+}]_{cyt}$ confined to the site of the Glu treatment, whereas AP was transmitted to distant cells (Koselski et al. 2020). This was rather an unexpected result because, in other plant species examined before, APs or variation potentials (known also as slow wave potentials, SWPs) spread together with Ca^{2+} waves and seem mutually dependent (Choi et al. 2014, 2017, Gilroy et al. 2016, Scherzer et al. 2022). In the model vascular plant *Arabidopsis thaliana*, two glutamate receptors (GLRs) *At*GLR3.3 and *At*GLR3.6 were identified as key players in wound-induced SWP generation and transmission (Mousavi et al. 2013, Farmer et al. 2020). Both genes are predominantly expressed in vascular tissues: phloem and xylem contact cells, respectively. Glu (and other amino acids) released from wounded tissues binds to the Ligand Binding Domain subunit of the GLR-like channels facilitating the opening of the channel pore and in consequence

Plant Cell Physiol. 64(8): 880–892 (2023) doi:https://doi.org/10.1093/pcp/pcad051, Advance Access publication on 26 May 2023, available online at https://academic.oup.com/pcp

initiating a Ca^{2+} wave and other downstream responses, like jasmonate (JA) key genes and other stress-related gene expressions (Grenzi et al. 2022).

According to the recent findings in vascular plants, in addition to the ion fluxes facilitating regenerative $[Ca^{2+}]_{cyt}$ wave formation and transmission, a ROS-based component supplements the long-distance signaling system (Baxter et al. 2014, Kurusu et al. 2015, Gilroy et al. 2016, Marcec et al. 2019). NADPH oxidases [respiratory burst oxidase homologs (RBOHs)] localized in the plasma membrane seem to be good candidates that fit with this scheme. RBOHs cause the reduction of oxygen to superoxide anion (O_2^-), which is quickly converted to hydrogen peroxide (H_2O_2). They possess EF-hand motifs that are activated upon binding of Ca^{2+} to enhance ROS production (Wojtaszek 1997, Marcec et al. 2019). Before the machinery of ROS scavenging reduces the ROS level back to normal, its temporary excess affects many metabolic and signaling pathways and their components. H_2O_2 produced in the apoplast can be quickly transported to the cytosol via aquaporins (Tian et al. 2016). Recently, a specific apoplastic H_2O_2 receptor, H_2O_2-Induced Ca^{2+} Increases 1 (HPCA1), was discovered (Wu et al. 2020). It is a membrane-spanning protein composed of an extracellular H_2O_2 sensor and a cytoplasmic kinase component, which is postulated to activate Ca^{2+}-permeable channels after H_2O_2 binding to the sensor (Foyer 2020, Wu et al. 2020). Thus, ion channels can be affected from both sides of the plasma membrane.

It was previously demonstrated that ROS can activate ion channels in different plant species classified in different branches of the phylogenetic tree of characean algae (Demidchik et al. 1997) to dicots and monocots (Wu et al. 2015). In vascular plants, H_2O_2 and hydroxyl radicals affect Ca^{2+}-permeable channels in the plasma membrane and in the internal store—the vacuole. In *A. thaliana*, two classes of non-selective calcium-permeable channels are postulated to be involved: GLR channels activated by Glu channel and cyclic nucleotide–gated channels (CNGCs; Finka et al. 2012, Mousavi et al. 2013). Additionally, annexin1 has been reported to be involved in ROS-induced $[Ca^{2+}]_{cyt}$ elevation (Richards et al. 2014). It has been demonstrated that homologs of Glu channels and CNGCs were involved in signaling processes in Physcomitrella (Finka and Goloubinoff 2014, Ortiz-Ramírez et al. 2017, Koselski et al. 2020).

In addition to calcium-permeable channels, K^+ channels in the plasma membrane have been found to respond to an increase in the ROS level (Demidchik et al. 2010). Massive K^+ efflux in ROS-treated plants was one of the first observations of plant response to this type of stress factors (Nassery 1979, Demidchik et al. 2010). In Arabidopsis, guard cell outward rectifying K^+ and stellar potassium outward rectifier channels have been identified to be responsible for that effect (Demidchik 2018). These channels are also regarded as good candidates to pass an outward current during the AP repolarization phase in excitable plants (Cuin et al. 2018, Scherzer et al. 2022).

The goal of our study was to examine for the first time the effect of the H_2O_2 application on long-distance electrical and calcium signaling systems in the model moss Physcomitrella. It was selected as a relatively simple plant, possessing no typical vascular tissues (Reski 1998), to address the question of evolution of signaling systems in early terrestrial plants. Electrical potential changes and $[Ca^{2+}]_{cyt}$ transients were measured in wild-type (WT) plants and *glr1*^{KO} mutants treated with H_2O_2. We demonstrated that in the WT plants, H_2O_2 evoked the electrical signals recorded both in the gametophyte leaves and protonema and the calcium signals predominantly in protonema. The susceptibility of the protonema to the treatment was much higher than in the leaf cells (0.5 mM versus 5 mM). These signals were blocked by La^{3+}—a calcium channel inhibitor—and by EDTA—a Ca^{2+} chelator. In the *glr1*^{KO} mutants, the electrical signals were reduced but not totally blocked, which reveals that GLR channels are not crucial in H_2O_2-induced membrane potential changes and Ca^{2+} fluxes in Physcomitrella. The involvement of other factors affecting $[Ca^{2+}]_{cyt}$ is discussed. Looking for the downstream effects of the signals, we demonstrate an enhanced expression of stress-related genes.

Results

Electrical signals in leaf cells

The microelectrode measurements carried out on leaf (phylloid) cells from the Physcomitrella gametophyte proved that the application of H_2O_2 evoked systemic electrical signals in the form of membrane potential changes transmitted along the plant. The long-distance responses transmitted from the basal part of the plant (from the rhizoid side) and recorded in apical leaf cells are presented in **Fig. 1A**. The different H_2O_2 concentrations influenced both the amplitude and the membrane potential characteristic of the response. Stimulation of the basal part of the plant with 0.05 mM and 0.1 mM H_2O_2 evoked irregular membrane potential changes with similar amplitude, duration and rate of depolarization (**Fig. 1A**, **Table 1**). After an increase of the H_2O_2 concentration to 0.5 mM, significant changes in basic parameters describing the membrane potential changes were obtained (**Fig. 1A**, **Table 1**). The cell membrane depolarized twice as fast as in the lower concentrations (14.5 ± 1.6 mV/s, $n = 18$) and reached more positive values. The amplitude of the depolarization (A) amounted to 68 ± 3 mV ($n = 19$) and was ~30 mV higher than after treatment with 0.05 and 0.1 mM H_2O_2, respectively. Another difference occurred in the shape of the responses, where after the peak of depolarization evoked by 0.5 mM H_2O_2, a several-minute plateau of the membrane potential was recorded.

We used H_2O_2 in the concentration of 0.5 mM to compare the transmission ability of electrical signals in the opposite direction—from the apical to the basal part of the plant (**Fig. 1B**). The electrical signals transmitted from the apical part of the plant characterized in a lower rate of

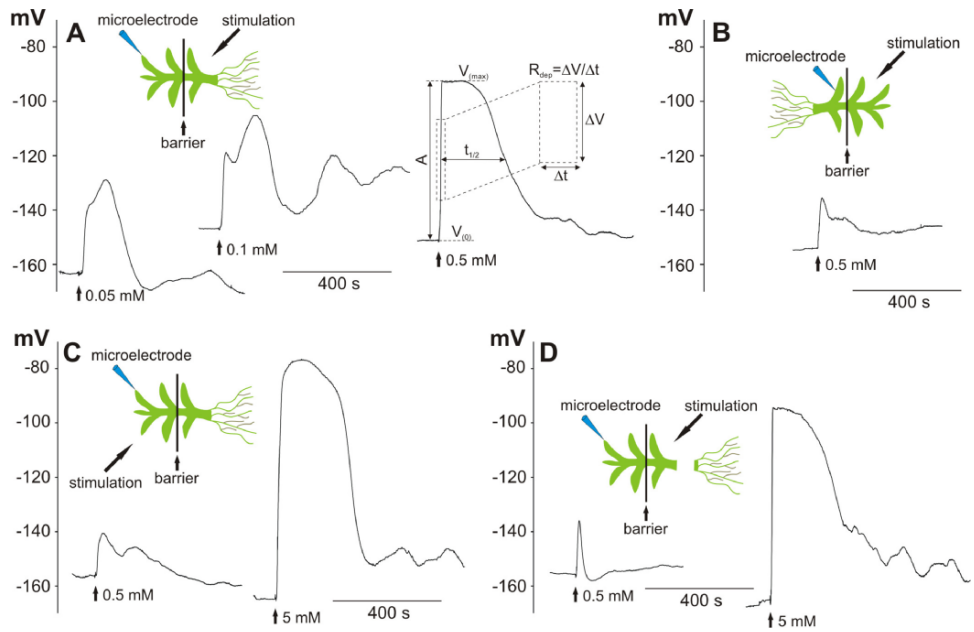

Fig. 1 H_2O_2-evoked long-distance electrical signals recorded in a Physcomitrella leaf (phylloid) cell. The recordings were carried out in bipartite chambers with a barrier separating two parts of the gametophyte. Schemes presenting the site of stimulation and insertion of the microelectrode are in placed on the top of the recordings. (A) Long-distance electrical signals in the form of membrane potential changes recorded after the stimulation of the basal part of the gametophyte with different H_2O_2 concentrations. The explanation of the method of obtaining parameters describing the membrane potential changes is shown. $V_{(0)}$—value of the membrane potential measured before the application of hydrogen peroxide, $V_{(max)}$—maximum value of the membrane potential recorded during the response, A—amplitude of the response, $t_{1/2}$—duration of the response measured in half of the amplitude, R_{dep}—depolarization rate measured in half of the amplitude on a section equal to the half of the amplitude. (B) Electrical signals recorded after stimulation of the apical part of the gametophyte. (C, D) Reduction of the sensitivity of the leaf cells to H_2O_2 recorded after direct stimulation of the tested cell located in the apical part of the gametophyte and in the gametophyte with a cutoff basal part, respectively. The vertical axes present the values of the membrane potential (in mV).

Table 1 Values of electrical signal parameters obtained in leaf cells after the application of H_2O_2 in different concentrations and different variants of experiments

	Membrane potential before stimulation $V_{(0)}$ (mV)	**Membrane potential at the peak of the response** $V_{(max)}$ (mV)	**Amplitude** A (mV)	**Duration at half of the peak** $t_{1/2}$ (s)	**Rate of depolarization** R_{dep} (mV/s)
Basal stimulation 0.5 mM	-154 ± 3 ($n = 19$)	$-86 \pm 3^{a,b,c,d,e}$ ($n = 19$)	$68 \pm 3^{a,b,c}$ ($n = 19$)	236 ± 44^{a} ($n = 17$)	$14.5 \pm 1.6^{a,b,c,d,e}$ ($n = 18$)
Basal stimulation 0.1 mM	-161 ± 4 ($n = 14$)	$-123 \pm 6^{d,i}$ ($n = 14$)	38 ± 6^{g} ($n = 14$)	169 ± 33 ($n = 13$)	6 ± 1.4^{e} ($n = 13$)
Basal stimulation 0.05 mM	-158 ± 2 ($n = 12$)	$-121 \pm 7^{e,j}$ ($n = 12$)	37 ± 6^{h} ($n = 12$)	140 ± 15 ($n = 11$)	4.4 ± 1^{d} ($n = 11$)
Apical stimulation 0.5 mM	-165 ± 5 ($n = 13$)	$-142 \pm 8^{a,f,k}$ ($n = 9$)	$22 \pm 5^{b,e,j}$ ($n = 9$)	$85 \pm 20^{c,f}$ ($n = 8$)	2.3 ± 0.4^{b} ($n = 8$)
Direct apical stimulation 0.5 mM	-153 ± 4 ($n = 9$)	$-136 \pm 7^{b,g,l}$ ($n = 9$)	$17 \pm 7^{a,d,i}$ ($n = 9$)	$89 \pm 28^{d,g}$ ($n = 8$)	2.9 ± 1.6^{a} ($n = 6$)
Direct apical stimulation 5 mM	-153 ± 5 ($n = 11$)	$-75 \pm 5^{f,g,h,i,j}$ ($n = 11$)	$78 \pm 4^{d,e,f,g,h}$ ($n = 11$)	$316 \pm 52^{e,f,g}$ ($n = 11$)	11.6 ± 3.5 ($n = 9$)
Basal stimulation of plant without rhizoids 0.5 mM	-156 ± 3 ($n = 15$)	$-130 \pm 7^{c,h,m}$ ($n = 12$)	$24 \pm 5^{c,f,k}$ ($n = 12$)	$51 \pm 12^{a,b,e}$ ($n = 12$)	3.3 ± 0.8^{c} ($n = 12$)
Basal stimulation of plant without rhizoids 5 mM	-153 ± 3 ($n = 10$)	$-86 \pm 6^{k,l,m}$ ($n = 10$)	$67 \pm 6^{i,j,k}$ ($n = 10$)	$389 \pm 79^{b,c,d}$ ($n = 9$)	10.5 ± 2.1 ($n = 10$)

Basal stimulation, apical stimulation, direct apical stimulation and basal stimulation of plants without rhizoids represent the variants of experiments presented in **Fig. 1A–D**, respectively. The values denote mean ± standard error. Dunn's test was performed for all pairwise comparisons ($P < 0.05$). $V_{(0)}$—value of the membrane potential measured before the application of hydrogen peroxide, $V_{(max)}$—maximum value of the membrane potential recorded during the response (at the peak of the response), A—amplitude of the response, $t_{1/2}$—duration of the response measured in half of the amplitude, R_{dep}—depolarization rate measured in half of the amplitude on a section equal to the half of the amplitude, n—number of tested plants.
Letters a-m indicate statistically significant differences.

depolarization ($R_{dep} = 2.3 \pm 0.4$ mV/s, $n = 8$), lower amplitude (22 ± 5 mV, $n = 9$) and lower voltage at the peaks of the signals ($V_{(max)} = -142 \pm 8$ mV, $n = 9$). The additional feature was an absence of a characteristic plateau of the membrane potential. The shape of the membrane potential changes resembled the responses obtained after direct stimulation of a cell in the apical

part of the plant (Fig. 1C) or removal of the basal part (Fig. 1D), where a 10-fold increase in the H_2O_2 concentration (to 5 mM) evoked responses similar to these transmitted from the basal part after 0.5 mM H_2O_2 administration. These results indicate that the highest susceptibility to H_2O_2 occurs in the basal part of the plant having protonema cells and rhizoids, which act as an initial place for the generation of long-distance electrical signals propagated toward the plant apex. The results also showed that an increase in the H_2O_2 concentration facilitates the generation of fully developed responses resembling APs.

APs belong to the basic long-distance electrical signals recorded in plant cells whose generation is dependent on an influx of calcium ions into the cytoplasm. We decided to study the dependence of the recorded responses on the presence of an inhibitor of calcium channels (2 mM lanthanum) or a calcium chelator (0.5 mM EDTA), respectively (Fig. 2A, B, Table 2). In addition to the effects of lanthanum and EDTA, we also examined the possibility to reverse the evoked effects. Each plant was stimulated twice—after initial immersion for 3–4 h in lanthanum or EDTA and then after the exchange of the solution back to the standard solution. Immersion of the plants in lanthanum caused a total blockage of the response in 10 of the 19 tested cells. The responses in the other plants had a significantly reduced amplitude (to 9 ± 2 mV, $n = 9$). Lanthanum also shifted the membrane potential ($V_{(0)}$) to positive values (to -130 ± 3 mV, $n = 19$). The depolarization after the lanthanum application was slower (R_{dep} amounted to 0.5 ± 0.2 mV/s, $n = 8$) and reached more negative values ($V_{(max)} = -128 \pm 5$, $n = 9$) than in the control plants. After a washout of lanthanum from the measuring chamber, the amplitude of the responses increased to 27 ± 4 mV ($n = 4$), which indicated that the inhibition of the responses by lanthanum is partially reversible. EDTA totally blocked the responses in 9 of the 18 tested cells. Similar to lanthanum, EDTA evoked the reduction of the amplitude (to 13 ± 4 mV, $n = 9$), the shift of the membrane potential to more positive values (to -122 ± 5 mV, $n = 18$) and the reduction of the rate of depolarization (to 1.4 ± 0.7 mV/s, $n = 7$). The shift of the membrane potential after EDTA was partially reversible since a washout resulted in a restoration of the membrane potential close to the values measured in standard solution (-144 ± 4 mV, $n = 18$).

Electrical signals in protonema cells

The results of the measurements carried out on the leaf cells indicated that it is hard to evoke electrical signals in such cells, and the responses can start mainly from the protonema cells and/or rhizoids—probably the target for the action of H_2O_2.

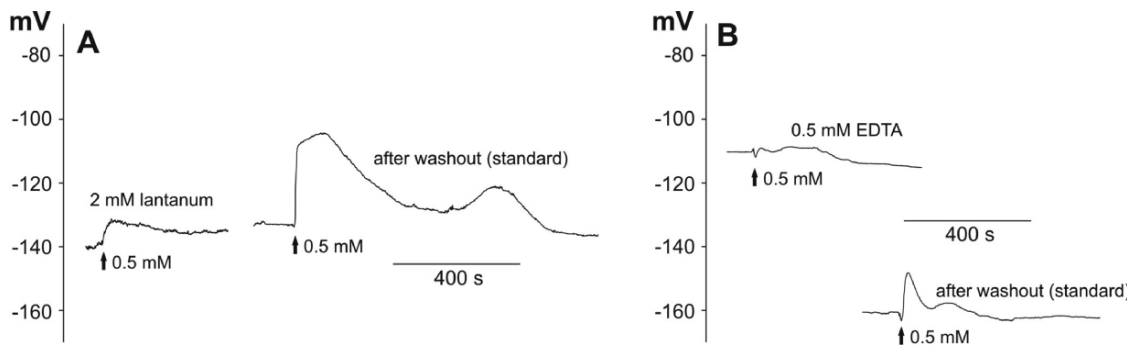

Fig. 2 Blockage of H_2O_2-evoked long-distance electrical signals by 2 mM lanthanum (A) and 0.5 mM EDTA (B). The method of stimulation was the same as in Fig. 1A. The representative membrane potential changes show the effects of preincubation in lanthanum (A) or EDTA (B), respectively, and then the washout of the drugs carried out on the same plant.

Table 2 Values of electrical signal parameters obtained in leaf cells after the application of 0.5 mM H_2O_2 in the basal part of the gametophyte

	Membrane potential before stimulation $V_{(0)}$ (mV)	**Membrane potential at the peak of the response** $V_{(max)}$ (mV)	**Amplitude** A (mV)	**Duration at half of the peak** $t_{1/2}$ (s)	**Rate of depolarization** R_{dep} (mV/s)
Standard (WT)	$-154 \pm 3^{a,b,c}$ ($n = 19$)	$-86 \pm 3^{a,b,c}$ ($n = 19$)	$68 \pm 3^{a,b,c,d}$ ($n = 19$)	236 ± 44 ($n = 17$)	$14.5 \pm 1.6^{a,b,c,d}$ ($n = 18$)
2 mM La^{3+}	-130 ± 3^{b} ($n = 19$)	$-128 \pm 5^{a,d}$ ($n = 9$)	$9 \pm 2^{a,e}$ ($n = 9$)	205 ± 25 ($n = 3$)	$0.5 \pm 0.2^{a,e}$ ($n = 8$)
After washout of 2 mM La^{3+}	-130 ± 4^{c} ($n = 19$)	-104 ± 5 ($n = 5$)	27 ± 4^{d} ($n = 4$)	224 ± 34 ($n = 15$)	3.6 ± 0.8^{c} ($n = 14$)
0.5 mM EDTA	$-122 \pm 5^{a,d,e}$ ($n = 18$)	-115 ± 7^{c} ($n = 9$)	13 ± 4^{b} ($n = 9$)	126 ± 32 ($n = 6$)	$1.4 \pm 0.7^{b,f}$ ($n = 7$)
After washout of 0.5 mM	-144 ± 4^{e} ($n = 18$)	-121 ± 7^{b} ($n = 8$)	24 ± 6^{c} ($n = 8$)	63 ± 14 ($n = 7$)	2.5 ± 0.7^{d} ($n = 7$)
Standard (Ppg*lr1*^{KO})	-146 ± 3^{d} ($n = 26$)	-100 ± 4^{d} ($n = 26$)	46 ± 3^{e} ($n = 26$)	194 ± 21 ($n = 25$)	$9.6 \pm 1.2^{e,f}$ ($n = 24$)

The responses recorded in the WT were obtained in the standard solution or the standard solution supplemented with 2 mM $LaCl_3$ or 0.5 mM EDTA. The *P. patens* knock-out mutants (Ppg*lr1*^{KO}) were tested in the standard solution. Explanations are provided in Table 1.
Letters a-f indicate statistically significant differences.

To study this hypothesis, we decided to examine the effect of H_2O_2 on membrane potential changes in protonema cells. In these measurements, stimulation was carried out by microinjection of H_2O_2 in three regions: initially into a chain of protonema cells adjacent to the tested cell with the inserted microelectrode, then directly into the tested cell and at the end into the gametophyte base.

The results confirmed that, although electrical signals in protonema cells are transmitted from cell to cell, the responses recorded in the same cell differed depending on the region of stimulation (**Fig. 4**, **Table 3**, **Supplementary Video S1**). The stimulation of the gametophyte base was the most effective, as it evoked electrical signals in each tested cell immediately upon stimulation. In comparison to the electrical signals recorded in the leaf cells, the signals from the protonema reached a higher amplitude (81 ± 4 mV, $n = 8$) and the duration measured in half of the amplitude ($t_{1/2} = 486 \pm 100$ s, $n = 8$). Surprisingly, weaker effects were achieved by the direct stimulation of the tested cell or the stimulation of adjacent cells located close to the tested cell. This method of stimulation evoked electrical signals with a smaller amplitude (66 ± 6 mV, $n = 8$) than when H_2O_2 was applied in the gametophyte base. The responses recorded in the protonema after the direct or indirect stimulation also exhibited a low depolarization rate (1.6 ± 0.6 mV/s, $n = 8$), compared to the responses in the basal part of the gametophyte (9.3 ± 2.5 mV/s, $n = 8$) or those recorded in the leaf cells. Cell-to-cell transmission of the electrical signal evoked by stimulation of the single protonema cells was rarely recorded and occurred only in 2 out of 18 tested plants (**Supplementary Fig. S1**, **Supplementary Video S2**).

One of the candidates responsible for cell-to-cell communication in plants is the GLR, which can act as a non-selective calcium-permeable channel. The participation of the GLR in the transmission of electrical signals recorded in our experiments was tested with the use of a *glr1* mutant of Physcomitrella (Pp*glr*^{KO}). In the Pp*glr1*^{KO} mutants, as in the WT, electrical signals propagated from the base of the gametophyte to the leaf and protonema cells (**Figs. 3**, **4**, **Supplementary Video S3**). In comparison to the WT, electrical signals recorded in the leaf cells of Pp*glr1*^{KO} had a reduced amplitude (to 46 ± 3 mV, $n = 26$) and a lower depolarization rate (9.6 ± 1.2 mV/s, $n = 24$). The amplitude and rate of depolarization of responses in the protonema cells from Pp*glr1*^{KO} recorded after the stimulation of the basal gametophyte part reached similar values to those recorded in the WT protonema cells (78 ± 3 mV, $n = 10$ and 8.9 ± 3 mV/s, $n = 10$, respectively). As in the WT protonema cells, the direct or indirect stimulation of the cells from Pp*glr1*^{KO} evoked a smaller amplitude (63 ± 4 mV, $n = 10$) and a lower depolarization rate (1.1 ± 0.3 mV/s, $n = 10$) than after the stimulation of the basal part of the Pp*glr1*^{KO} gametophyte. All these changes in the parameters of membrane potential changes in the protonema cells are presented in **Table 3**.

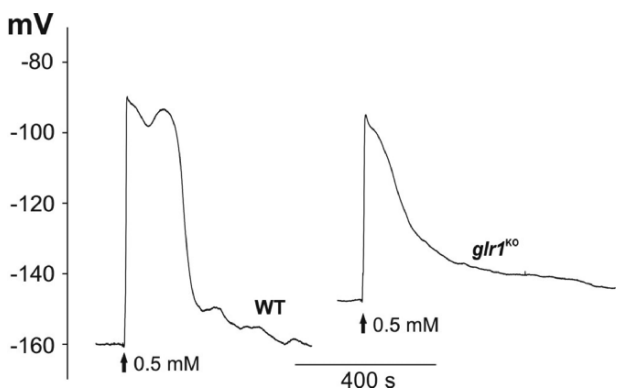

Fig. 3 Comparison of H_2O_2-evoked long-distance electrical signals recorded in the WT and the Pp*glr1*^{KO} mutant. The method of stimulation was the same as in **Fig. 1A**.

Calcium signals

Calcium signals were recorded in plants expressing GCaMP3, i.e. a fluorescent calcium indicator. Fluorescence measurements of calcium signals recorded after the stimulation of the basal part of the plant indicated that the application of 0.5 mM H_2O_2 evoked calcium waves which propagated from cell to cell in thread-like protonema cells. In contrast to electrical signals, the calcium signals were slower and appeared a few minutes after the application of the stimulus (**Fig. 5**, **Supplementary Video S4**). In some plants, the calcium signals did not start at the stimulation site but appeared at some distance from the stimulation, acting as a new source for calcium waves. In such a situation, calcium wave propagation was observed in both directions—into and from the stimulation site. The rate of calcium signal propagation along the protonema toward the site of the stimulation was similar to that in the opposite direction, reaching 5.5 ± 0.7 μm/s ($n = 4$) and 5.2 ± 0.3 μm/s ($n = 7$), respectively. A characteristic trait of some recorded calcium signals was its decrement with distance (**Supplementary Fig. S2**, **Supplementary Video S5**). As in the case of electrical signals, the observation of calcium signals in the stimulated leaves was possible after the increase of the H_2O_2 concentration to 5 mM (**Supplementary Video S6**). In turn, in contrast to electrical signals, calcium signals in leaf cells after the application of 0.5 mM H_2O_2 to the basal part of the plant were observed occasionally only in several cells from single leaves but never (in none of 30 tested plants) in all leaves (**Supplementary Video S7**).

Expression of genes in distant regions of the moss

To analyze whether the electrical signal that was triggered upon local treatment would be accompanied by changes in gene expressions in distant tissues, we selected candidate genes and performed quantitative real-time PCR (qPCR). The candidates were selected based on homology to Arabidopsis genes differentially expressed after local stress stimulus (Zandalinas et al. 2019). In that study, a high light stimulus was locally imposed on selected Arabidopsis rosette leaves, and changes in gene expression in the locally treated and distant, non-treated leaves (local and systemic responses, respectively) were

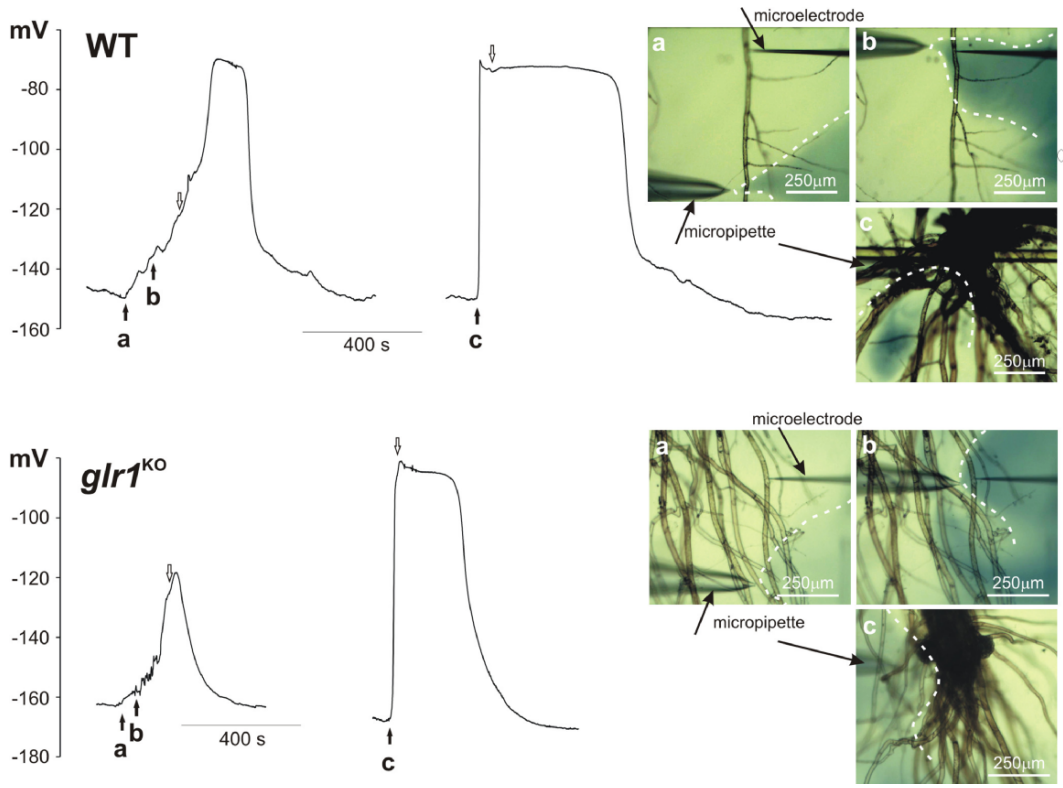

Fig. 4 H_2O_2-evoked membrane potential changes recorded in protonema cells from the WT and the Pp*glr1*^{KO} mutant. H_2O_2 (0.5 mM) was injected into the selected site by the micropipette. In the pictures placed on the right side of the presented traces, three different measurement variants are presented: a—stimulation of the cells adjacent to the tested cell (site of the microelectrode insertion), b—direct stimulation of the tested cell and c—stimulation of the basal part of the gametophyte. The pictures show dispersion of H_2O_2 stained with 1 mM aniline blue (marked by dashed white lines) recorded 5 s after time points a, b and c marked on the trace by the black arrows. The end of stimulation (removal of the micropipette from the measuring chamber) was marked by the white arrows.

Table 3 Values of parameters of electrical signals in protonema cells after the application of 0.5 mM H_2O_2 directly/indirectly to the cell or in the basal part of the gametophyte

	Membrane potential before stimulation $V_{(0)}$ (mV)	**Membrane potential at the peak of the response $V_{(max)}$ (mV)**	**Amplitude A (mV)**	**Duration at half of the peak $t_{1/2}$ (s)**	**Rate of depolarization R_{dep} (mV/s)**
Direct/indirect stimulation (WT)	-155 ± 8 ($n = 8$)	-89 ± 9 ($n = 8$)	66 ± 6 ($n = 8$)	403 ± 105 ($n = 7$)	$1.6 \pm 0.6^{a,d}$ ($n = 8$)
Basal stimulation (WT)	$-155 \pm 7^{d,h}$ ($n = 8$)	-74 ± 4 ($n = 8$)	81 ± 4^{a} ($n = 8$)	486 ± 100 ($n = 8$)	$9.3 \pm 2.5^{a,b}$ ($n = 8$)
Direct/indirect stimulation (Pp*glr*^{KO})	-146 ± 4 ($n = 10$)	-84 ± 5 ($n = 10$)	63 ± 4^{a} ($n = 10$)	300 ± 70 ($n = 10$)	$1.1 \pm 0.3^{b,c}$ ($n = 10$)
Basal stimulation (Pp*glr1*^{KO})	-155 ± 2 ($n = 10$)	-77 ± 3 ($n = 10$)	78 ± 3 ($n = 10$)	294 ± 25 ($n = 9$)	$8.9 \pm 3^{c,d}$ ($n = 10$)

Direct stimulation and indirect stimulation correspond to the measuring variants presented in **Fig. 4**. Letters a-d indicate statistically significant differences. Explanations are provided in **Table 1**.
Letters a-h indicate statistically significant differences.

investigated by RNAseq analysis. From this published list, we selected candidate genes that were upregulated in the systemic response if their expression was also inducible via H_2O_2 treatment and depended on the function of the RBOH D (RBOHD). Here, the gene encoding a galacturonosyltransferase-like 10 protein (AT3G28340) was 5-fold upregulated 5 min after the light stress treatment (Zandalinas et al. 2019). In Physcomitrella, we identified four homologous proteins (Pp3c5_28420V3.1, Pp3c25_14930V3.1, Pp3c16_25090V3.1 and Pp3c2_18670V3.1) via *BlastP* search (Altschul et al. 1997) against the Physcomitrella proteome (Lang et al. 2018). In analogy to Zandalinas et al. (2019), we tested their responsiveness to H_2O_2 treatment and submerged entire gametophores in 0.5 mM H_2O_2 for 8 min. Here, we employed hydroponic gametophore cultures and analyzed the expression of the candidate genes with qPCR. Of the four Physcomitrella homologs, only

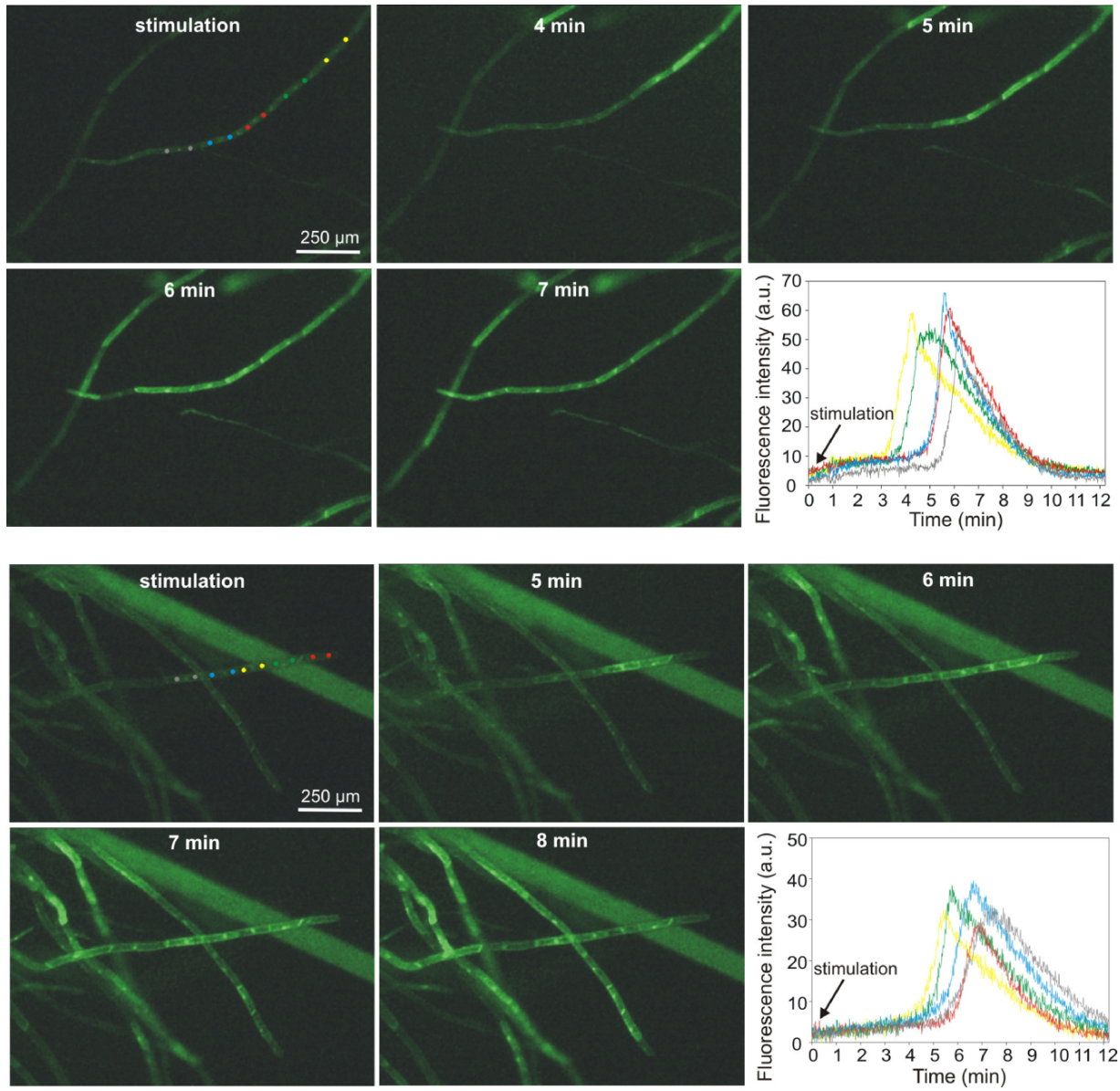

Fig. 5 H_2O_2-evoked calcium signals recorded in protonema cells expressing fluorescent calcium biosensor GCaMP3. For each cell, two circular regions of interest (ROIs) located in the cytoplasmic region from both sides of the nucleus were analyzed. The two panels of pictures show two different types of calcium signal propagation—at the upper panel, the signal propagates in one direction starting from the site of stimulation (basal part of the gametophyte), and at the lower panel, the signal propagation starts from one cell (marked by yellow ROIs) and propagates in two opposite directions. The changes in fluorescence intensity in different ROIs are presented in the bottom right corner of each picture panel.

one gene (**Supplementary Fig. S3**, Pp3c16_25090V3.1) exhibited a significant increase in gene expression ($P = 0.0305$) and hence was selected for further analysis. For Pp3c5_28420V3.1, an increase in gene expression was detectable (**Supplementary Fig. S3**), but the difference was not significant. Nevertheless, this gene was included in further experiments.

For these two selected candidates, we tested whether both genes are regulated in gametophore sections distant from a local treatment with H_2O_2. Apices of gametophores were harvested after treatment with 0.5 mM H_2O_2 at the base for 8 min (**Supplementary Fig. S4**), as well as corresponding untreated apices. A significant upregulation of Pp3c16_25090V3.1 ($P = 0.00184$) was observed (**Fig. 6**), whereas an upregulation of Pp3c5_28420V3.1 was indicated but was not statistically significant ($P = 0.06075$). Thus, a local stress stimulus (here H_2O_2 at the gametophore base) triggers alteration of gene expression within 8 min in distant sections (here apex) in Physcomitrella.

Discussion

Plant cell signaling is based mainly on the generation and transmission of different types of signals including electrical,

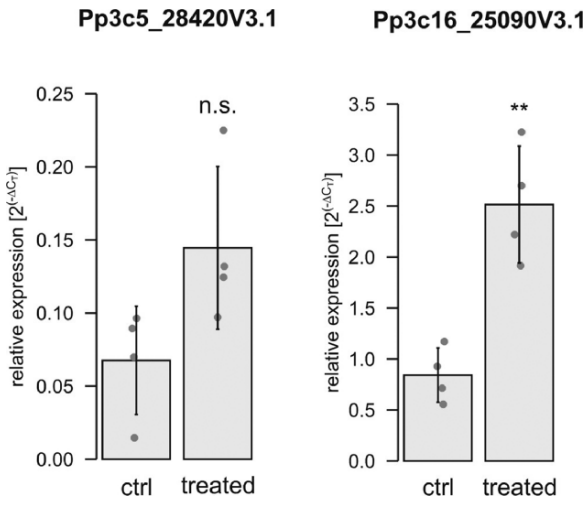

Fig. 6 Gene expression analysis by qPCR of the selected gene candidates. Apices were used from untreated gametophores and gametophores treated at the base with 0.5 mM H_2O_2 for 8 min. Dots represent biological replicates (mean values from three technical replicates). Bars are the mean values from the four biological replicates with standard deviation. Relative expression ($2^{(-\Delta CT)}$) of Pp3c5_28420V3.1 and Pp3c16_25090V3.1 is calculated against the reference genes L21 (Pp3c13_2360V3.1) and LWD (Pp3c22_18860V3.1) according to Livak and Schmittgen (2001). Significance levels are based on a one-way ANOVA with subsequent Tukey's HSD post hoc test (**$P < 0.01$); n.s. = not significant.

calcium and ROS. Investigations of the relationship between these signals allow unraveling signaling pathways triggered in response to biotic and abiotic stresses. In this study, we tried to answer the question of whether the external application of ROS (H_2O_2) evokes a systemic response in the form of electrical and calcium signals to analyze the interdependence of these signals and their impact on gene expression in distant regions.

The importance of ROS in the plant defense system has been evidenced by many experiments (Huang et al. 2019). One of the first studies focused on the involvement of ROS in cell-to-cell communication in *Arabidopsis* (Miller et al. 2009) proved that local stimuli produced ROS waves propagating through the plant at a rate of 8.4 cm/min and the response was dependent on the *RBOHD* gene encoding plant NADPH oxidase involved in the production of ROS. The rate of propagation of such RBOHD-related ROS signals recorded in different tissues ranged from ∼400 to 1400 μm/s and was dependent on the type of stress (Choi et al. 2017). The accumulation of extracellular ROS was observed along the path of propagation (Miller et al. 2009), indicating that each cell along the path is able to activate RBOHD and release ROS in adjacent cells. In such an auto-propagation process, named ROS-induced ROS release, H_2O_2 generated by RBOHD can be regarded as a long-distance signal. However, in the study by Miller et al. (2009), the external application of H_2O_2 did not evoke a ROS wave indicating the involvement of some other signal molecules in the propagation of the ROS wave.

Calcium is a candidate for such a signal molecule and, together with ROS, can cooperate in long-distance transmission of information about stimuli. For example, calcium-dependent protein kinase CPK5 playing a role in plant immunity is important for cell-to-cell communication based on ROS waves (Dubiella et al. 2013). There are also other ways of activation of RBOH proteins by calcium, including direct binding of this ion to the EF-hand motif on the RBOH protein (Kimura et al. 2012) or binding of phosphatidic acid to the same protein whose accumulation in the cell can be induced by calcium (Zhang et al. 2009). In addition to the calcium-induced ROS release process, ROS-induced calcium release is possible. For example, it has been shown that ROS can activate different calcium-permeable channels, e.g. hyperpolarization-activated Ca^{2+} channels in root cells (Demidchik et al. 2007), Ca^{2+} influx channels in guard cells (Pei et al. 2000) or Ca^{2+}-permeable channels regulated by annexin1 (Richards et al. 2014). Recent studies carried out on Arabidopsis allowed the discovery of a plasma membrane leucine-rich repeat receptor kinase, i.e. HPCA1, which links the perception of apoplastic H_2O_2 with Ca^{2+} signaling (Wu et al. 2020). One of the most probable mechanisms for the cooperation between calcium and ROS in long-distance transmission of signals is that an increase in cytoplasmic calcium evoked by a local stimulus can induce the production of ROS via Ca^{2+}–RBOH interactions and the accumulation of ROS in the apoplast. The transport of ROS from the apoplast to the cell, probably carried out by aquaporins, would evoke ROS-induced calcium release, which in turn could induce ROS production (Gilroy et al. 2014).

As shown by the results of our study, H_2O_2-evoked calcium signals are not systemic responses, such as those observed earlier in *P. patens* under osmotic stress or salt stimulation (Storti et al. 2018). Calcium waves with a velocity of ∼400 μm/s in response to local salt stress were also recorded in Arabidopsis (Choi et al. 2014), where the blockage of calcium channels by lanthanum inhibited not only the calcium waves but also the ROS-regulated transcriptional marker (ZAT12), indicating that calcium and ROS waves are closely linked. Assuming the interconnection of calcium signals and ROS waves, it is unlikely that the extracellular application of H_2O_2 in our experiments evoked the ROS wave since the H_2O_2-evoked calcium signals admittedly appeared at some distance from the stimulation site but propagated with a decrement (**Fig. 5**, **Supplementary Videos S4 and S5**, **Supplementary Fig. S2**). The other feature of the H_2O_2-evoked calcium signals in Physcomitrella, i.e. the slower rate of propagation than in the case of the ROS wave (>5 μm/s), also indicates a low probability of the appearance of a calcium-associated ROS wave. The ability to evoke local calcium signals but not self-propagating calcium waves by the extracellular H_2O_2 application implies the engagement of some other factors taking part in the transmission of information about such stimuli. It seems that, in *P. patens*, electrical signals, which appear at the moment of stimulation and propagate along the whole plant, are a proper carrier of the information

about H_2O_2 enhancement. There still remains the question of the relationships between electrical, calcium and ROS signals.

The relationship between ROS and electrical signals was previously confirmed in Arabidopsis mutants lacking RBOHD, where propagating electrical signals after heat stress or high light had a significantly reduced amplitude or were totally blocked (Suzuki et al. 2013). Taking into account the ability of extracellular ROS (mainly H_2O_2) to activate different ion channels (Demidchik 2018), including calcium-permeable channels that can participate in long-distance electrical signals, it seems that ROS can promote electrical signals along the ROS wave path. This hypothesis can also be supported by the similar velocity of different types of plant self-propagating electrical signals to the velocity of the ROS wave [like APs (20–400 cm/min) and system potentials (5–10 cm/min); Zimmermann et al. 2009]. In Physcomitrella, the H_2O_2-evoked electrical signals propagated immediately from the basal part along the whole plant (**Figs. 1**, **4**, **Supplementary Video S1**), indicating that the signals appeared before the slowly propagating calcium waves. In cooperation with ROS and calcium waves, electrical signals, which are probably the fastest carriers of information, can initiate the whole array of plant defense responses. It is also probable that, by reaching cells distant from the stimulation site, electrical signals initiate a calcium wave response only in some cells, in which the threshold of calcium signal generation is lower than in other cells. This assumption is proved by the observation of calcium waves in the protonema cells, where, at a distance from the stimulation site in the basal part of the plant, only a few protonema cells in the thread-like chain generated calcium signals propagating in two directions—into and out of the site of stimulation (**Fig. 5**, **Supplementary Fig. S2**, **Supplementary Videos S4 and S5**).

One of the candidates for ion channels participating in long-distance electrical signals in plants is GLR-like channels, which was confirmed in experiments carried out on Arabidopsis (Mousavi et al. 2013, Salvador-Recatalà et al. 2014, Salvador-Recatalà 2016). Wound-induced electrical signals recorded in this species were dependent on clade III GLRs (GLR 3.3 and GLR 3.6) and played a crucial role in the distal production of JAs taking part in plant defense responses (Mousavi et al. 2013). It is a matter of discussion if those channels are directly responsible for Ca^{2+} fluxes since they are predominantly expressed in endomembranes (Nguyen et al. 2018, Farmer et al. 2020).

In Physcomitrella, only two *GLR* genes have been identified (Verret et al. 2010). Both genes (*PpGLR1* and *PpGLR2*) are paralogs to *GLR* clade III from Arabidopsis (De Bortoli et al. 2016) and encode channels participating in chemotaxis and reproduction of Physcomitrella (Ortiz-Ramírez et al. 2017). A patch-clamp study indicated that GLR1 is a calcium-permeable ion channel localized in the cell membrane and partially inhibited by GLR antagonists (Ortiz-Ramírez et al. 2017). These data indicate that GLR1 in Physcomitrella, similar to GLR 3.3 and GLR 3.6 from Arabidopsis, can be important in the transmission of long-distance electrical signals. This hypothesis was not fully confirmed in our study since H_2O_2 evoked long-distance electrical signals in the Physcomitrella *glr1*^{KO} mutants (**Figs. 3**, **4**, **Supplementary Video S3**); however, the response differed in the amplitude (**Table 2**). Such a 'weak' effect of the GLR1 knockout suggests that, in addition to GLR channels, other channels must be engaged in the long-distance propagation of ROS-induced electrical signals. The most important channels taking part in the generation of electrical signals in Physcomitrella are probably calcium permeable, given the blockage of H_2O_2-evoked responses by the calcium channel inhibitor (lanthanum) or the calcium chelator (EDTA) (**Fig. 2**). It is also probable that, in addition to ion channels in the plasma membrane, a significant role in the transmission of electrical signals is assigned to intracellular calcium channels. One of the best-known intracellular channels permeable, e.g., to calcium is the two-pore channel 1 (TPC1) located in the vacuolar membrane, the tonoplast (Dadacz-Narloch et al. 2011). A patch-clamp study carried out in our laboratory demonstrated that TPC channels in Physcomitrella vacuoles conduct Ca^{2+} currents (Koselski et al. 2013). Involvement of the channel in the transmission of long-distance calcium waves has been demonstrated (Choi et al. 2014), but there is no information about the role of TPC1 in the transmission of electrical signals. As calcium-permeable channels, TPC1 may be involved in the release of calcium from intracellular compartments (Qudeimat et al. 2008) leading to calcium-induced calcium release (CICR), a desired phenomenon for long-distance signal transmission, but this assumption arouses controversy (Ward and Schroeder 1994, Pottosin et al. 1997). The role of H_2O_2 in CICR is questionable since microelectrode ion flux estimation and patch-clamp studies carried out on vacuoles from *Beta vulgaris* demonstrated that H_2O_2 suppressed the Ca^{2+} efflux from the vacuole and slow vacuolar currents carried by TPC1 (Pottosin et al. 2009).

Effectively, the treatment with 0.5 mM H_2O_2 at the base of gametophores was sufficient to trigger an increase in gene expression in the apex of a component of the homogalacturonan biosynthesis (**Fig. 6**, Pp3c16_25090V3.1). Here, the homologous candidate Pp3c5_28420V3.1 was not significantly upregulated although an increasing trend was detectable. This agrees with publicly available data, indicating that both genes are not co-expressed. Galacturonosyltransferase-like proteins such as Pp3c16_25090V3.1 act in the pectin assembly (homogalacturonan biosynthesis) of the primary cell wall (reviewed by Loix et al. 2017). Under oxidative stress, cell wall pectins also represent a source for the biosynthesis of ascorbic acid (Valpuesta and Botella 2004, García-Caparrós et al. 2021), which in turn is used to detoxify ROS such as H_2O_2. Both selected candidates are homologs of an Arabidopsis isoform (AT3G28340) whose gene expression is regulated via ROS waves (Zandalinas et al. 2019). However, it should be noted that Galacturonosyltransferase-like proteins comprise a large gene family with at least 21 members in Arabidopsis and 17 genes in Physcomitrella (Van Bel et al. 2022) and clear ortholog relations are not yet resolved. The expression of the Arabidopsis homolog (AT3G28340) was 5-fold increased only in systemic leaves distant from a local high light stress impulse (Zandalinas et al. 2019), and those data further

indicate that the increase of expression was a response to a ROS wave. In contrast, the two selected homologs in Physcomitrella were not regulated by high light stress (**Supplementary Fig. S5**), but their expression increased after heat stress. Heat stress in plants is accompanied by the elevated production of ROS such as H_2O_2 (reviewed by Mittler et al. 2022). In summary, these data show that the gene expression of at least one of the two Physcomitrella candidates (Pp3c16_25090V3.1) is responsive to ROS. Consequently, the increase of expression in the untreated apex (**Fig. 6**) was likely based on a propagating ROS wave.

Taken together, our study demonstrates differences in the generation and propagation of H_2O_2-evoked electrical and calcium signals in the model moss Physcomitrella. Many of the applied variants of measurements indicated that the basal part of the gametophyte is the most excitable region, probably because a large number of protonema cells are juvenile cells from an early stage of new gametophyte development. In comparison to the leaf cells, the responses in the protonema exhibited higher amplitudes and lasted longer, which may indicate higher susceptibility of such cells to ROS (**Tables 2** and **3**, **Figs. 1**, **4**). The main difference between the electrical and calcium signals was the velocity of propagation, which was higher in the electrical signals. The other difference was the ability to propagate without a decrement; in contrast to the electrical signals, calcium signals diminished with distance, even if they appeared at some distance from stimuli (**Supplementary Fig. S2**, **Supplementary Video S5**). Given these differences, we propose that H_2O_2-evoked long-distance electrical signals are the first to reach distant regions of the plant and activate calcium signals, but not in every cell. The protonema cells were the most susceptible to calcium signals, indicating that the signals play a key role in young and developing cells. A similar observation was reported in our previous work focused on Glu-evoked calcium signals (Koselski et al. 2020). Electrical and calcium signals were not the only effect of H_2O_2 application. Gene expression analysis proved that apart from the signals, an increase of stress-related gene expression is observed in not stimulated distant regions of plants (**Fig. 6**). The increase in the gene expression appeared after 8 min—the time close to the duration of electrical signals. The similar time scale of electrical signals and gene expression raises the question about interdependence of both phenomena.

Materials and Methods

Cultivation of plant material used for electrophysiological and calcium imaging analysis

Physcomitrella gametophytes were grown on Knop solid agar medium (Reski and Abel 1985) in 160-mm diameter Petri dishes. The WT plants and knockout *glr1* mutants (Pp*glr1*^{KO}) were used for the analysis of membrane potential changes in leaf and protonema cells with the use of the microelectrode technique. A Physcomitrella mutant expressing GCaMP3 was used for the fluorescence imaging of changes in the calcium concentration. The plants were grown in a growing chamber (Conviron Adaptis A1000, Conviron, Winnipeg, Canada) at a photoperiod of 16-/8-h light/dark, with light intensity 50 μmol/m^2 s and at a temperature set to 23°C.

Cultivation of plant material used for gene expression analysis

Physcomitrella WT protonema [new species name: *P. patens* (Hedw.) Mitt.; Medina et al. 2019] ecotype 'Gransden 2004' was cultivated in Knop medium with microelements (MEs). Knop medium (pH 5.8) containing 250 mg/l KH_2PO_4, 250 mg/l KCl, 250 mg/l $MgSO_4 \times 7\ H_2O$, 1,000 mg/l $Ca(NO_3)_2 \times 4\ H_2O$ and 12.5 mg/l $FeSO_4 \times 7\ H_2O$ was prepared as described by Reski and Abel (1985), and 10 mL per liter of an ME stock solution (309 mg/l H_3BO_3, 845 mg/l $MnSO_4 \times 1\ H_2O$, 431 mg/l $ZnSO_4 \times 7\ H_2O$, 41.5 mg/l KI, 12.1 mg/l $Na_2MoO_4 \times 2\ H_2O$, 1.25 mg/l $CoSO_4 \times 5\ H_2O$ and 1.46 mg/l $Co(NO_3)_2 \times 6\ H_2O$) was also prepared as described by Egener et al. (2002) and Schween et al. (2003). The suspension culture was dispersed weekly with an ULTRA-TURRAX (IKA, Staufen, Germany) at 18,000 rpm for 90 s.

Hydroponic cultures of Physcomitrella gametophores were cultivated as described by Hoernstein et al. (2023). Glass rings covered with mesh (PP, 250-m mesh, 215-m thread, Zitt-Thoma GmbH, Freiburg, Germany) were prepared as described by Erxleben et al. (2012). Protonema suspension was adjusted to a final density of 440 mg/l (dry weight per volume) as described by Decker et al. (2017) and evenly distributed in equal volumes on the mesh surface. Glass rings covered with protonema were placed in Magenta® vessels (Sigma-Aldrich, St. Louis, MO, USA). KnopME medium was supplemented until it touched the bottom of the mesh. The medium was changed every 4 weeks.

Suspension cultures and hydroponic cultures were cultivated in standard light conditions (55 μmol photons/m^{2}s) at 22°C in a 16-/8-h light/dark cycle.

Measurements of membrane potential in leaf cells

The method of membrane potential measurements with microelectrodes was similar to that employed by Koselski et al. (2020). Plastic Petri dishes used in the microelectrode measurements were divided into two chambers with a barrier. The barrier had a small (1-mm width) gap sealed with Vaseline. Before the experiments, the plants were incubated for 3–6 h at a light intensity of 50 μmol/m^2 in a bath solution containing (in mM) 1 KCl, 1 $CaCl_2$, 50 sorbitol and 2 HEPES, pH 7.5 (buffered by Tris). The stimuli were introduced by the application of 500 μl of a bath solution supplemented with 0.5 mM H_2O_2. The lanthanum chloride or EDTA influence on the H_2O_2-evoked responses described in this study was assessed by the application of one of these substances into one of the Petri dish compartments containing the basal part of the plant. Borosilicate glass capillaries (1B150F-6, World Precision Instruments, Sarasota, FL, USA) were used to make micropipettes with the use of a P-30 micropipette puller (Sutter Instrument Co., Novato, CA, USA), filled with 100 mM KCl and connected to the FD223 electrometer (World Precision Instruments, Sarasota, FL, USA). A Sensapex SMX (SensApex, Oulu, Finland) electronic micromanipulator was used for positioning and insertion of the microelectrode. The reference electrode was composed of an Ag/$AgCl_2$ wire inside a plastic tube filled with 100 mM KCl and ending with a porous tip. The measured data were acquired by a Lab-Trax-4 device (World Precision Instruments, Sarasota, FL, USA) working with LabScribe2 software, which also allowed analyses of the data. The analysis of statistical differences was performed in SigmaStat 4.0 (Systat Software Inc., Palo Alto, CA, USA). Recordings of changes in the membrane potential were recorded with a 2-Hz data collection frequency. Figures were prepared with the use of Sigma Plot 9.0 (Systat Software Inc, California, USA) and CorelDraw 12 (Corel Corporation, Ottawa, Canada) software.

Measurements of membrane changes in protonema cells

The plants were prepared in the same way as for the measurements carried out on the leaves. The ME was positioned and inserted using a PatchStar (Scientifica, East Sussex, UK) micromanipulator and observed under an Olympus IX71 (Olympus, Tokyo, Japan) microscope with a camera (Artcam-500MI, Tokyo, Japan) working with QuickPHOTO Camera software (version 2.3, Promicra, Prague, Czech Republic). A CellTram Vario microinjector (Eppendorf, Hamburg,

Germany) with a borosilicate glass micropipette (with a diameter of ~3 μm) was used for the application of H_2O_2 onto the cell surface. As in our previous paper (Koselski et al. 2020), 1 mM methyl blue was used for staining of the stimulating solution, which allows the observation of its dispersion. Live recording of membrane potentials visible in LabScribe 3 software and microscope camera images were recorded by Open Broadcaster Software (ver. 23.2.1; Open Broadcaster Software, Massachusetts, USA).

Fluorescence calcium imaging

Films and images of calcium concentration changes in the GCaMP3 *P. patens* mutants were recorded with the use of NIS-Elements AR software (ver. 5.20.00; Nikon, Tokyo, Japan) working with a Nikon Eclipse Ti fluorescence microscope equipped with a Nikon Plan UW 2× WD:7.5 objective and a Nikon DS-Ri2 camera (Nikon, Tokyo, Japan). The excitation of fluorescence was provided by a Prior lumen 200 metal arc lamp (Prior Scientific Instruments Ltd, Cambridge, England) and a 495-nm dichroic mirror with a standard GFP excitation filter 470 ± 20 nm. Images of fluorescence emission were recorded with 1-s exposure and a standard GFP fluorescence emission barrier filter 525 ± 50 nm (Nikon, Tokyo, Japan). Stimulation of the plants was carried out by microinjection using a CellTram Vario microinjector (Eppendorf, Hamburg, Germany). The standard solution supplemented with H_2O_2 was visible due to tinting by 0.025 μM fluorescein.

Treatment of plants used for gene expression analysis

Gametophores from hydroponic cultures were used for the treatment with H_2O_2. Half of the gametophores from one glass ring were cut approximately in the middle, and only the upper half of the gametophores (~100 mg) was used as a control sample. Cut gametophore apices were gently dried by dabbing with filter paper. The glass ring with the remaining uncut gametophores was transferred into a new Magenta® vessel containing KnopME with 0.5 mM H_2O_2. After 8 min, the upper half of the remaining uncut gametophores (treated sample) was harvested as described earlier. In total, gametophores from four independent hydroponic cultures (four biological replicates) were sampled.

RNA extraction and qPCR

Extraction of RNA was done with the innuPREP Plant RNA Kit (Analytic Jena, Jena, Germany) using the extraction buffer 'PL'. Of the total RNA, 5 μg was treated with DNAseI (Thermo Fisher Scientific, Waltham, MA, USA) at 37°C for 1 h, and integrity of the RNA was checked on agarose gels. Two-microgram DNAseI digested RNA was used for reverse transcription using the TaqMan™ Reverse Transcription kit (N8080234, Thermo Fisher Scientific) with random hexamer primers. Reverse transcription was performed at 42°C for 1 h. A non-transcribed control without the addition of MultiScribe™ Reverse Transcriptase enzyme was included. Primers for the qPCR were designed using the Primer3Plus software (https://www.primer3plus.com/; Untergasser et al. 2012) with qPCR settings, and an efficiency of 2 was confirmed using a 1:2 dilution series of cDNA. Melting curve analysis was performed to exclude the presence of off-targets. qPCR was performed in 96-well plates using the SensiFast™ SYBR No-ROX Kit (Bioline, Memphis, Tennessee, USA) in technical triplicates for each biological replicate. Fifty-nanogram cDNA was used for each technical triplicate, and the PCR reaction was performed in a LightCycler® 480 (Roche, Basel, Switzerland). –RT and water controls for each primer pair were included. The PCR reaction was performed in 45 cycles with a melting temperature of 60°C. The expression analysis of the genes *Pp3c5_28420V3* and *Pp3c16_25090V3* [genes of interest (GOIs)] was performed as described by Bohlender et al. (2020) in relation to the housekeeping (reference) genes *L21* coding for the ribosomal protein L21 (*Pp3c13_2360V3*, Beike et al. 2015) and *LWD* coding for the transducin/WD40 repeat-like superfamily protein (*Pp3c22_18860V3*, Schuessele et al. 2016). All primers are listed in **Supplementary Table S1**. The expression levels were calculated relative to the reference genes according to Livak and Schmittgen (2001) using the software for the LightCycler® 480 (V1.5.0, Roche, Basel, Switzerland). Relative expression is represented as $2^{(-\Delta CT)}$ with $\Delta CT = CT_{[GOI]} - CT_{[reference]}$. **Fig. 6** is created and statistics were calculated in R (R Core Team 2022). Statistical significance was tested via one-way ANOVA with subsequent Tukey's honest significant difference (HSD) post hoc test. Significance was accepted at $P < 0.05$.

Supplementary Data

Supplementary data are available at *PCP* online.

Data Availability

The data underlying this article are available in the article and in its online supplementary material. The other data underlying this article will be shared on request to the corresponding author.

Funding

National Science Centre, Poland (DAINA 1, 2017/27/L/NZ1/03164); German Research Foundation under Germany's Excellence Strategy (CIBSS-EXC-2189, Project ID 390939984).

Acknowledgments

The authors thank Prof. José A. Feijó, Dr. Jörg D. Becker and Dr. Mário R. Santos for sharing the GLR1 knock-out mutant of Physcomitrella. The authors thank Dr. Thomas J. Kleist for providing the transgenic lines of Physcomitrella expressing GCaMP3. We thank Richard Haas for performing the qPCR experiments and Anne Katrin Prowse for language editing.

Author Contribution

M.K. conceived and designed the manuscript, prepared the main part of experiments, analyzed and interpreted the data and drafted the main part of the work. P.W. participated in the preparation of the membrane potential measurements. K.T. participated in writing and revising the manuscript. S.N.W.H and R.R. designed qPCR experiments, analyzed the data and helped in writing the manuscript.

Disclosures

The authors have no conflicts of interest to declare.

References

Altschul, S.F., Madden, T.L., Schäffer, A.A., Zhang, J., Zhang, Z., Miller, W., et al. (1997) Gapped BLAST and PSI-BLAST: a new generation of protein database search programs. *Nucleic Acids Res.* 25: 3389–3402.

Baxter, A., Mittler, R. and Suzuki, N. (2014) ROS as key players in plant stress signalling. *J. Exp. Bot.* 65: 1229–1240.

Beike, A.K., Lang, D., Zimmer, A.D., Wüst, F., Trautmann, D., Wiedemann, G., et al. (2015) Insights from the cold transcriptome of *Physcomitrella*

patens: global specialization pattern of conserved transcriptional regulators and identification of orphan genes involved in cold acclimation. *New Phytol.* 205: 869–881.

Bohlender, L.L., Parsons, J., Hoernstein, S.N.W., Rempfer, C., Ruiz-Molina, N., Lorenz, T., et al. (2020) Stable protein sialylation in *Physcomitrella*. *Front. Plant Sci.* 11: 1–21.

Choi, W.G., Miller, G., Wallace, I., Harper, J., Mittler, R. and Gilroy, S. (2017) Orchestrating rapid long-distance signaling in plants with Ca^{2+}, ROS and electrical signals. *Plant J.* 90: 698–707.

Choi, W.G., Toyota, M., Kim, S.H., Hilleary, R. and Gilroy, S. (2014) Salt stress-induced Ca^{2+} waves are associated with rapid, long-distance root-to-shoot signaling in plants. *Proc. Natl. Acad. Sci. U.S.A.* 111: 6497–6502.

Cuin, T.A., Dreyer, I. and Michard, E. (2018) The role of potassium channels in *Arabidopsis thaliana* long distance electrical signalling: AKT2 modulates tissue excitability while GORK shapes action potentials. *Int. J. Mol. Sci.* 19: 1–17.

Dadacz-Narloch, B., Beyhl, D., Larisch, C., López-Sanjurjo, E.J., Reski, R., Kuchitsu, K., et al. (2011) A novel calcium binding site in the slow vacuolar cation channel TPC1 senses luminal calcium levels. *Plant Cell* 23: 2696–2707.

De Bortoli, S., Teardo, E., Szabò, I., Morosinotto, T. and Alboresi, A. (2016) Evolutionary insight into the ionotropic glutamate receptor superfamily of photosynthetic organisms. *Biophys. Chem.* 218: 14–26.

Decker, E.L., Alder, A., Hunn, S., Ferguson, J., Lehtonen, M.T., Scheler, B., et al. (2017) Strigolactone biosynthesis is evolutionarily conserved, regulated by phosphate starvation and contributes to resistance against phytopathogenic fungi in a moss, *Physcomitrella patens*. *New Phytol.* 216: 455–468.

Demidchik, V. (2018) ROS-activated ion channels in plants: biophysical characteristics, physiological functions and molecular nature. *Int. J. Mol. Sci.* 19: 1–18.

Demidchik, V., Cuin, T.A., Svistunenko, D., Smith, S.J., Miller, A.J., Shabala, S., et al. (2010) Arabidopsis root K^+-efflux conductance activated by hydroxyl radicals: single-channel properties, genetic basis and involvement in stress-induced cell death. *J. Cell. Sci.* 123: 1468–1479.

Demidchik, V., Shabala, S.N. and Davies, J.M. (2007) Spatial variation in H_2O_2 response of *Arabidopsis thaliana* root epidermal Ca^{2+} flux and plasma membrane Ca^{2+} channels. *Plant J.* 49: 377–386.

Demidchik, V., Sokolik, A. and Yurin, V. (1997) The effect of Cu^{2+} on ion transport systems of the plant cell plasmalemma. *Plant Physiol.* 114: 1313–1325.

Dubiella, U., Seybold, H., Durian, G., Komander, E., Lassig, R., Witte, C.P., et al. (2013) Calcium-dependent protein kinase/NADPH oxidase activation circuit is required for rapid defense signal propagation. *Proc. Natl. Acad. Sci. U.S.A.* 110: 8744–8749.

Egener, T., Granado, J., Guitton, M.C., Hohe, A., Holtorf, H., Lucht, J.M., et al. (2002) High frequency of phenotypic deviations in *Physcomitrella patens* plants transformed with a gene-disruption library. *BMC Plant Biol.* 2: 1–9.

Erxleben, A., Gessler, A., Vervliet-Scheebaum, M. and Reski, R. (2012) Metabolite profiling of the moss *Physcomitrella patens* reveals evolutionary conservation of osmoprotective substances. *Plant Cell Rep.* 31: 427–436.

Farmer, E.E., Gao, Y.Q., Lenzoni, G., Wolfender, J.L. and Wu, Q. (2020) Wound- and mechanostimulated electrical signals control hormone responses. *New Phytol.* 227: 1037–1050.

Finka, A., Cuendet, A.F.H., Maathuis, F.J.M., Saidi, Y. and Goloubinoff, P. (2012) Plasma membrane cyclic nucleotide gated calcium channels control land plant thermal sensing and acquired thermotolerance. *Plant Cell* 24: 3333–3348.

Finka, A. and Goloubinoff, P. (2014) The CNGCb and CNGCd genes from *Physcomitrella patens* moss encode for thermosensory calcium channels responding to fluidity changes in the plasma membrane. *Cell Stress Chaperones* 19: 83–90.

Foyer, C.H. (2020) Making sense of hydrogen peroxide signals. *Nature* 578: 518–519.

Frank, W., Ratnadewi, D. and Reski, R. (2005) *Physcomitrella patens* is highly tolerant against drought, salt and osmotic stress. *Planta* 220: 384–394.

García-Caparrós, P., De Filippis, L., Gul, A., Hasanuzzaman, M., Ozturk, M., Altay, V., et al. (2021) Oxidative stress and antioxidant metabolism under adverse environmental conditions: a review. *Bot. Rev.* 87: 421–466.

Gilroy, S., Białasek, M., Suzuki, N., Górecka, M., Devireddy, A.R., Karpiński, S., et al. (2016) ROS, calcium, and electric signals: key mediators of rapid systemic signaling in plants. *Plant Physiol.* 171: 1606–1615.

Gilroy, S., Suzuki, N., Miller, G., Choi, W.G., Toyota, M., Devireddy, A.R., et al. (2014) A tidal wave of signals: calcium and ROS at the forefront of rapid systemic signaling. *Trends Plant Sci.* 19: 623–630.

Grenzi, M., Bonza, M.C. and Costa, A. (2022) Signaling by plant glutamate receptor-like channels: what else! *Curr. Opin. Plant Biol.* 68: 1–9.

Hoernstein, S.N.W., Özdemir, B., van Gessel, N., Miniera, A.A., Rogalla von Bieberstein, B., Nilges, L., et al. (2023) A deeply conserved protease, acylamino acid-releasing enzyme (AARE), acts in ageing in *Physcomitrella* and *Arabidopsis*. *Commun. Biol.* 6: 1–16.

Huang, H., Ullah, F., Zhou, D.X., Yi, M. and Zhao, Y. (2019) Mechanisms of ROS regulation of plant development and stress responses. *Front. Plant Sci.* 10: 1–10.

Kimura, S., Kaya, H., Kawarazaki, T., Hiraoka, G., Senzaki, E., Michikawa, M., et al. (2012) Protein phosphorylation is a prerequisite for the Ca^{2+}-dependent activation of Arabidopsis NADPH oxidases and may function as a trigger for the positive feedback regulation of Ca^{2+} and reactive oxygen species. *Biochim. Biophys. Acta Mol. Cell Res.* 1823: 398–405.

Koselski, M., Trebacz, K. and Dziubinska, H. (2013) Cation-permeable vacuolar ion channels in the moss *Physcomitrella patens*: a patch-clamp study. *Planta* 238: 357–367.

Koselski, M., Trebacz, K., Dziubinska, H. and Krol, E. (2008) Light- and dark-induced action potentials in *Physcomitrella patens*. *Plant Signal. Behav.* 3: 13–18.

Koselski, M., Wasko, P., Derylo, K., Tchorzewski, M. and Trebacz, K. (2020) Glutamate-induced electrical and calcium signals in the moss *Physcomitrella patens*. *Plant Cell Physiol.* 61: 1807–1817.

Koselski, M., Wasko, P., Kupisz, K. and Trebacz, K. (2019) Cold- and menthol-evoked membrane potential changes in the moss *Physcomitrella patens*: influence of ion channel inhibitors and phytohormones. *Physiol. Plant.* 167: 433–446.

Kurusu, T., Kuchitsu, K. and Tada, Y. (2015) Plant signaling networks involving Ca^{2+} and Rboh/Nox-mediated ROS production under salinity stress. *Front. Plant Sci.* 6.

Lang, D., Ullrich, K.K., Murat, F., Fuchs, J., Jenkins, J., Haas, F.B., et al. (2018) The *Physcomitrella patens* chromosome-scale assembly reveals moss genome structure and evolution. *Plant J.* 93: 515–533.

Livak, K.J. and Schmittgen, T.D. (2001) Analysis of relative gene expression data using real-time quantitative PCR and the $2^{-\Delta\Delta CT}$ method. *Methods* 25: 402–408.

Loix, C., Huybrechts, M., Vangronsveld, J., Gielen, M., Keunen, E. and Cuypers, A. (2017) Reciprocal interactions between cadmium-induced cell wall responses and oxidative stress in plants. *Front. Plant Sci.* 8: 1–19.

Marcec, M.J., Gilroy, S., Poovaiah, B.W. and Tanaka, K. (2019) Mutual interplay of Ca^{2+} and ROS signaling in plant immune response. *Plant Sci.* 283: 343–354.

Medina, R., Johnson, M.G., Liu, Y., Wickett, N.J., Shaw, A.J. and Goffinet, B. (2019) Phylogenomic delineation of *Physcomitrium* (Bryophyta: Funariaceae) based on targeted sequencing of nuclear exons and their flanking regions rejects the retention of *Physcomitrella*, *Physcomitridium* and *Aphanorrhegma*. *J. Syst. Evol.* 57: 404–417.

Miller, G., Schlauch, K., Tam, R., Cortes, D., Torres, M.A., Shulaev, V., et al. (2009) The plant NADPH oxidase RBOHD mediates rapid systemic signaling in response to diverse stimuli. *Sci. Signal* 2: 1–10.

Mittler, R., Zandalinas, S.I., Fichman, Y. and Van Breusegem, F. (2022) Reactive oxygen species signalling in plant stress responses. *Nat. Rev. Mol. Cell Biol.* 23: 663–679.

Mousavi, S.A.R., Chauvin, A., Pascaud, F., Kellenberger, S. and Farmer, E.E. (2013) GLUTAMATE RECEPTOR-LIKE genes mediate leaf-to-leaf wound signalling. *Nature* 500: 422–426.

Nassery, H. (1979) Salt-induced loss of potassium from plant roots. *New Phytol.* 83: 23–27.

Nguyen, C.T., Kurenda, A., Stolz, S., Chételat, A. and Farmer, E.E. (2018) Identification of cell populations necessary for leaf-to-leaf electrical signaling in a wounded plant. *Proc. Natl. Acad. Sci. U.S.A.* 115: 10178–10183.

Ortiz-Ramírez, C., Michard, E., Simon, A.A., Damineli, D.S.C., Hernández-Coronado, M., Becker, J.D., et al. (2017) GLUTAMATE RECEPTOR-LIKE channels are essential for chemotaxis and reproduction in mosses. *Nature* 549: 91–95.

Pei, Z.M., Murata, Y., Benning, G., Thomine, S., Klüsener, B., Allen, G.J., et al. (2000) Calcium channels activated by hydrogen peroxide mediate abscisic acid signalling in guard cells. *Nature* 406: 731–734.

Pottosin, I.I., Tikhonova, L.I., Hedrich, R. and Schönknecht, G. (1997) Slowly activating vacuolar channels can not mediate Ca^{2+}-induced Ca^{2+} release. *Plant J.* 12: 1387–1398.

Pottosin, I., Wherrett, T. and Shabala, S. (2009) SV channels dominate the vacuolar Ca^{2+} release during intracellular signaling. *FEBS Lett.* 583: 921–926.

Qudeimat, E., Faltusz, A.M.C., Wheeler, G., Lang, D., Brownlee, C., Reski, R., et al. (2008) A PIIB-type Ca^{2+}-ATPase is essential for stress adaptation in *Physcomitrella patens*. *Proc. Natl. Acad. Sci. U.S.A.* 105: 19555–19560.

R Core Team (2022) R: A Language and Environment for Statistical Computing. R Foundation for Statistical Computing, Vienna, Austria.

Rensing, S.A., Goffinet, B., Meyberg, R., Wu, S.Z. and Bezanilla, M. (2020) The moss *Physcomitrium* (*Physcomitrella*) *patens*: a model organism for non-seed plants. *Plant Cell* 32: 1361–1376.

Rensing, S.A., Lang, D., Zimmer, A.D., Terry, A., Salamov, A., Shapiro, H., et al. (2008) The *Physcomitrella* genome reveals evolutionary insights into the conquest of land by plants. *Science* 319: 64–69.

Reski, R. (1998) Development, genetics and molecular biology of mosses. *Bot. Acta* 111: 1–15.

Reski, R. and Abel, W.O. (1985) Induction of budding on chloronemata and caulonemata of the moss, *Physcomitrella patens*, using isopentenyladenine. *Planta* 165: 354–358.

Richards, S.L., Laohavisit, A., Mortimer, J.C., Shabala, L., Swarbreck, S.M., Shabala, S., et al. (2014) Annexin 1 regulates the H_2O_2-induced calcium signature in *Arabidopsis thaliana* roots. *Plant J.* 77: 136–145.

Saidi, Y., Finka, A., Muriset, M., Bromberg, Z., Weiss, Y.G., Maathuis, F.J.M., et al. (2009) The heat shock response in moss plants is regulated by specific calcium-permeable channels in the plasma membrane. *Plant Cell* 21: 2829–2843.

Salvador-Recatalà, V. (2016) New roles for the GLUTAMATE RECEPTOR-LIKE 3.3, 3.5, and 3.6 genes as on/off switches of wound-induced systemic electrical signals. *Plant Signal. Behav.* 11: 1–10.

Salvador-Recatalà, V., Tjallingii, W.F. and Farmer, E.E. (2014) Real-time, in vivo intracellular recordings of caterpillar-induced depolarization waves in sieve elements using aphid electrodes. *New Phytol.* 203: 674–684.

Scherzer, S., Böhm, J., Huang, S., Iosip, A.L., Kreuzer, I., Becker, D., et al. (2022) A unique inventory of ion transporters poises the Venus flytrap to fast-propagating action potentials and calcium waves. *Curr. Biol.* 32: 4255–4263.

Schuessele, C., Hoernstein, S.N.W., Mueller, S.J., Rodriguez-Franco, M., Lorenz, T., Lang, D., et al. (2016) Spatio-temporal patterning of arginyl-tRNA protein transferase (ATE) contributes to gametophytic development in a moss. *New Phytol.* 209: 1014–1027.

Schween, G., Hohe, A., Koprivova, A. and Reski, R. (2003) Effects of nutrients, cell density and culture techniques on protoplast regeneration and early protonema development in a moss, *Physcomitrella patens*. *J. Plant Physiol.* 160: 209–212.

Storti, M., Costa, A., Golin, S., Zottini, M., Morosinotto, T. and Alboresi, A. (2018) Systemic calcium wave propagation in *Physcomitrella patens*. *Plant Cell Physiol.* 59: 1377–1384.

Suzuki, N., Miller, G., Salazar, C., Mondal, H.A., Shulaev, E., Cortes, D.F., et al. (2013) temporal-spatial interaction between reactive oxygen species and abscisic acid regulates rapid systemic acclimation in plants. *Plant Cell* 25: 3553–3569.

Tian, S., Wang, X., Li, P., Wang, H., Ji, H., Xie, J., et al. (2016) Plant aquaporin AtPIP1;4 links apoplastic H_2O_2 induction to disease immunity pathways. *Plant Physiol.* 171: 1635–1650.

Tucker, E.B., Lee, M., Alli, S., Sookhdeo, V., Wada, M., Imaizumi, T., et al. (2005) UV-A induces two calcium waves in *Physcomitrella patens*. *Plant Cell Physiol.* 46: 1226–1236.

Untergasser, A., Cutcutache, I., Koressaar, T., Ye, J., Faircloth, B.C., Remm, M., et al. (2012) Primer3-new capabilities and interfaces. *Nucleic Acids Res.* 40: 1–12.

Valpuesta, V. and Botella, M.A. (2004) Biosynthesis of L-ascorbic acid in plants: new pathways for an old antioxidant. *Trends Plant Sci.* 9: 573–577.

Van Bel, M., Silvestri, F., Weitz, E.M., Kreft, L., Botzki, A., Coppens, F., et al. (2022) PLAZA 5.0: extending the scope and power of comparative and functional genomics in plants. *Nucleic Acids Res.* 50: D1468–D1474.

Verret, F., Wheeler, G., Taylor, A.R., Farnham, G. and Brownlee, C. (2010) Calcium channels in photosynthetic eukaryotes: implications for evolution of calcium-based signalling. *New Phytol.* 187: 23–43.

Ward, J. and Schroeder, J.I. (1994) Calcium-activated K^+ channels and calcium-induced calcium release by slow vacuolar ion channels in guard cell vacuoles implicated in the control of stomatal closure. *Plant Cell* 6: 669–683.

Wojtaszek, P. (1997) Mechanisms for the generation of reactive oxygen species in plant defence response. *Acta Physiol. Plant.* 4: 581–589.

Wu, F., Chi, Y., Jiang, Z., Xu, Y., Xie, L., Huang, F., et al. (2020) Hydrogen peroxide sensor HPCA1 is an LRR receptor kinase in *Arabidopsis*. *Nature* 578: 577–581.

Wu, H., Shabala, L., Zhou, M. and Shabala, S. (2015) Chloroplast-generated ROS dominate NaCl-induced K^+ efflux in wheat leaf mesophyll. *Plant Signal. Behav.* 10: 1–4.

Zandalinas, S.I., Sengupta, S., Burks, D., Azad, R.K. and Mittler, R. (2019) Identification and characterization of a core set of ROS wave-associated transcripts involved in the systemic acquired acclimation response of *Arabidopsis* to excess light. *Plant J.* 98: 126–141.

Zhang, Y., Zhu, H., Zhang, Q., Li, M., Yan, M., Wang, R., et al. (2009) Phospholipase Dα1 and phosphatidic acid regulate NADPH oxidase activity and production of reactive oxygen species in ABA-mediated stomatal closure in *Arabidopsis*. *Plant Cell* 21: 2357–2377.

Zimmermann, M.R., Maischak, H., Mithöfer, A., Boland, W. and Felle, H.H. (2009) System potentials, a novel electrical long-distance apoplastic signal in plants, induced by wounding. *Plant Physiol.* 149: 1593–1600.